Geometry modifications and alignment of H_2O in an intense femtosecond laser pulse

J. H. Sanderson,[1] A. El-Zein,[1] W. A. Bryan,[1] W. R. Newell,[1] A. J. Langley,[2] and P. F. Taday[2]
[1]*Department of Physics and Astronomy, University College London, Gower Street, London WC1E 6BT, England*
[2]*Central Laser Facility, Rutherford Appleton Laboratory, Chilton, Didcot, Oxfordshire OX11 0QX, England*
(Received 13 August 1998)

The Coulomb explosion of H_2O in laser pulses of 50 fs and intensity of 3×10^{16} W/cm^2 has been investigated using an ion momentum-imaging technique to determine the shape of the exploding molecule. The molecule is found to straighten substantially during the ionization process with the bend distribution at a maximum between 130° and 180°. [S1050-2947(99)50904-9]

PACS number(s): 33.80.Rv, 33.80.Gj, 33.90.+h

Modifications to the structure of a small molecule during laser-induced Coulomb explosion is an active area of interest at present. Experiments have shown that the bond lengths of polyatomic molecules as large as SF_6 [1] expand to double their normal value before multiple ionization is complete. Evidence has been found to support bending of both the ground state [2,3,4] and vibrationally excited [5] CO_2 molecule, and straightening of the initially bent SO_2 molecule [6]. A more recent experiment indicated that SO_2 retains its bent structure [7] for high ionization channels. In the present experiment we use a momentum-imaging technique developed by Hishikawa *et al.* [7] to examine the modification to the initially bent H_2O molecule in a 50-fs laser pulse of peak intensity 3×10^{16} W/cm^2.

The 790-nm, 10-Hz laser used in the present experiment has been modified from that used in earlier studies [1,4,5]. The incident laser beam enters the vacuum system, which has a base pressure of 10^{-9} Torr, through a fused silica window and is reflection focused using an $f/5$ spherical mirror into the interaction region, which gives a near-diffraction-limited Gaussian spot radius, calculated to be 2.5 μm. The intensity was derived from the spot size and the pulse energy of 900 μJ to peak at 3×10^{16} W/cm^2. The direction of the laser polarization was controlled using a half-wave plate. The laser focus was situated in a central plane equidistant from two parallel grids separated by 20 mm, which formed the source region of a Wiley-McLaren–type time-of-flight (TOF) mass spectrometer [8], in which a 3-mm aperture was placed in front of the microchannel plates [4]. During the experiment the target gas pressure rose to 10^{-7} Torr and because of the increase in both the laser pulse energy and the focal spot size, the signal strength was one hundred times higher than in previous work [4]. The signal from the channel plates was therefore fed directly into a Tektronix TDS 744A digital oscilloscope interfaced to a personal computer. The laser pulses were monitored as previously [4] in order to minimize the effect of energy fluctuations. The polarization was rotated in 2° steps and a TOF spectrum was recorded at each step. Only one hundred laser pulses were needed to build up each spectrum and so a two-dimensional matrix of TOF spectra from 0° to 360° could be built up in approximately 30 min. The intensity distribution of an ion as a function of momentum, $I(P)$, is derived for each TOF spectrum, using the formula $P=\epsilon q\Delta T$, where q is the ion charge, ϵ is the extraction field strength, and ΔT is the flight time relative to the known flight time of an ion with zero initial momentum. A momentum map is then created by combining the distributions in polar form to give the signal strength as a function of momentum and angle with respect to the laser polarization direction.

Figures 1(a)–1(c) show momentum maps [7] of the observed atomic fragment ions, H^+, O^+, and O^{2+} constructed from spectra recorded at 2° intervals from 0° to 360°. The vertical axis is parallel to the laser polarization direction. Clear information can be gained from these plots. Figure 1(a) shows a low-momentum island ($<10\times10^3$ amu ms^{-1}) con-

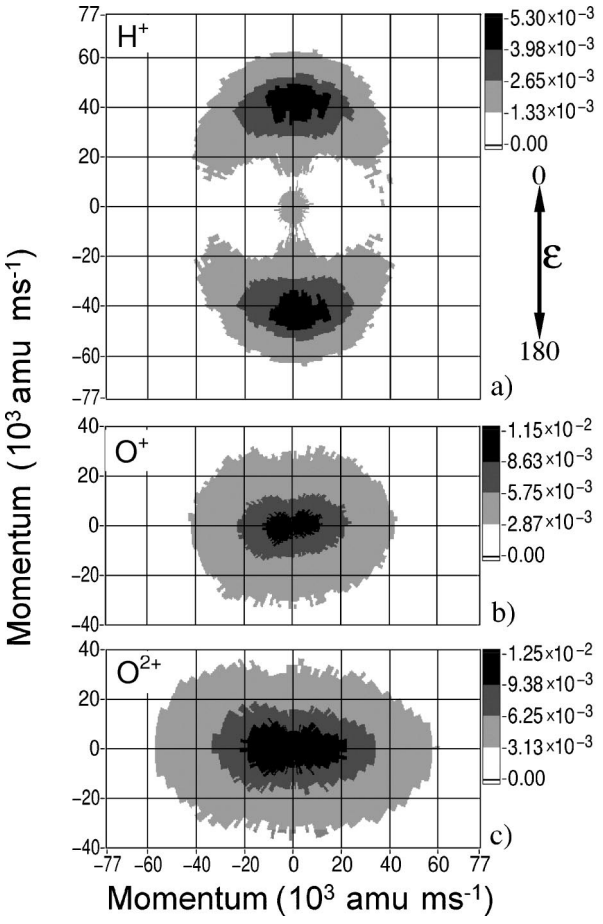

FIG. 1. Momentum maps for the atomic fragment ions resulting from the Coulomb explosion of H_2O. The vertical axis is parallel to the laser field direction ϵ.

sisting of ions from the $H^+ + OH$ (1,0) channel. The island is circular, indicating that the angular distribution of these ions is isotropic. The crescent-shaped islands, which consist of ions from the Coulomb channels (1,1,1) and (1,2,1), have a wide angular distribution, but are not isotropic. The gray intensity scale shows that these islands have their highest values at angles close to 0° and 180°, which indicates that the Coulomb explosions result from H_2O molecules in which a certain amount of alignment exists between the H-H axis and the laser polarization direction. We have fitted a function of the form $A\cos^n\theta$ to the H^+ angular distribution, at a momentum of 40×10^3 amu ms^{-1}, which is close to the highest point on the island (at 0° and 180°). The least-squares fit gives a value of $n=4.5$, which compares with $n=12$ for the (1,1,1) channel of CO_2 at the same laser intensity [4]. We can try to explain the observations of both the low- and high-momentum hydrogen fragments by considering a number of important results.

Recent experiments with laser pulses of less than 100 fs and intensity greater than 10^{14} W/cm^2 have shown that the angular distributions of fragments from light diatomic molecules cannot be explained simply by the higher ionization rate of molecules, which are initially aligned with the laser field [9,10]. This indicates that the laser field reorients light diatomic molecules on a femtosecond time scale. By contrast it was found that the massive I_2 molecule could not be reoriented on such a short time scale. The H_2O molecule is light and so it is reasonable to assume that the origin of the angular distribution, observed here, is the reorientation of the H_2O molecule by the laser field. The static-field-induced dipole strengths parallel and perpendicular to the H-H axis have recently been calculated for a range of field strengths [11]. These calculations suggest that at low laser intensity ($\approx10^{13}$ W/cm^2), the torques on the molecule associated with these dipoles are roughly equal and opposite, so that the molecule is not reoriented. The angular distributions of H^+ ions, most probably from the (1,0) channel, were measured in that work and found to be isotropic. This observation is confirmed in the present work, as the low-momentum H^+ ions must originate from a region within the focal spot where the intensity is low enough to result in only single ionization channels such as (1,0). The calculations further showed that at higher intensities, the parallel-induced dipole becomes dominant and so the molecule should be rotated, such that the H-H axis aligns with the laser field. This prediction is confirmed by the present result. The effect of opposing torques should reduce the amount of reorientation experienced by the molecule in comparison with more linear molecules such as CO_2, leading to a lower value of n as observed here. Furthermore, the bent nature of H_2O is important in widening the angular distribution of the Coulomb channel in a very simple way. If the H-H axis is completely aligned with the polarization direction, the trajectories of the H^+ ions cannot be along the polarization direction, because of the repulsion from the laterally offset oxygen ion. The bent nature of H_2O is deducible from Figs. 1(b) and 1(c) in which the O^+ and O^{2+} momentum plots are elliptical. In both cases the major axis of the ellipse is orientated at 90° to the laser polarization direction. This indicates that the molecules aligned with the H-H axis along the polarization direction repel the central oxygen ion at right angles to the polarization direction; this is only possible from a bent geometry.

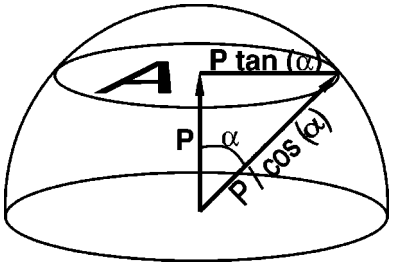

FIG. 2. Correction geometry used for the finite collection angle α of the detector. P is the momentum parallel to the detector axis and the signal measured at a particular P is proportional to the area $A=\pi(P\tan\alpha)^2$; see text for discussion.

Further information about the molecular geometry can be extracted from the momentum maps, but first it is necessary to correct the data for the effect of the variation of detector acceptance angle with ion momentum. This variation has the most effect on the oxygen ion maps in Figs. 1(b) and 1(c), because the momenta of the oxygen fragments are small, and so the acceptance angle becomes large, reaching $\pi/2$ for momenta close to zero. This means that the ion distributions appear more isotropic than is physically the case. Figure 2 shows the geometry, which must be considered for the correction procedure applied to each momentum point P on the map. In Fig. 2 the signal S measured at a particular momentum P is proportional to the momentum surface area A, defined by $\pi(P\tan\alpha)^2$, where α is the acceptance angle of the most energetic ion, which can be detected with momentum $P/\cos(\alpha)$ and which can be calculated from the experimental geometry. The measured signal is divided by the factor $\pi\sin^2(\alpha)$, which is analogous to a solid angle correction. A fuller discussion of this and other correction procedures will be given elsewhere.

Figures 3(a)–3(c) show the angular distributions of H^+, O^+, and O^{2+}, respectively, after a correction for the variation of acceptance angle. In Fig. 3(a) the central island is now not visible, but the Coulomb islands have not been greatly altered, as their momentum is high. The major difference is in Figs. 3(b) and 3(c) where removing the false isotropy has transformed the elliptical islands into ''bow-tie''-shaped islands. It is now possible to use the three corrected maps to deduce the geometry of the exploding molecule, by comparing them with maps derived from a Monte Carlo simulation of the Coulomb explosion of the H_2O molecule from a distribution of geometries. A similar technique has been used previously [3] to determine molecular geometry from the islands of a double correlation map. In the present simulation, three independent distributions are chosen to represent the O—H bond length R, the H—O—H bond angle θ, and the alignment angle ϕ between the H-H axis and the laser polarization direction. The distributions used are either triangles or trapeziums for ease of calculation. The simulated O^+ map was derived from a set of R, θ, and ϕ distributions in which the molecule was allowed to explode into the (1,1,1) channel and the O^{2+} map was derived from a set of distributions in which the molecule exploded into the (1,2,1) channel. The simulated H^+ map contains contributions from both channels, weighted in accordance with the magnitudes

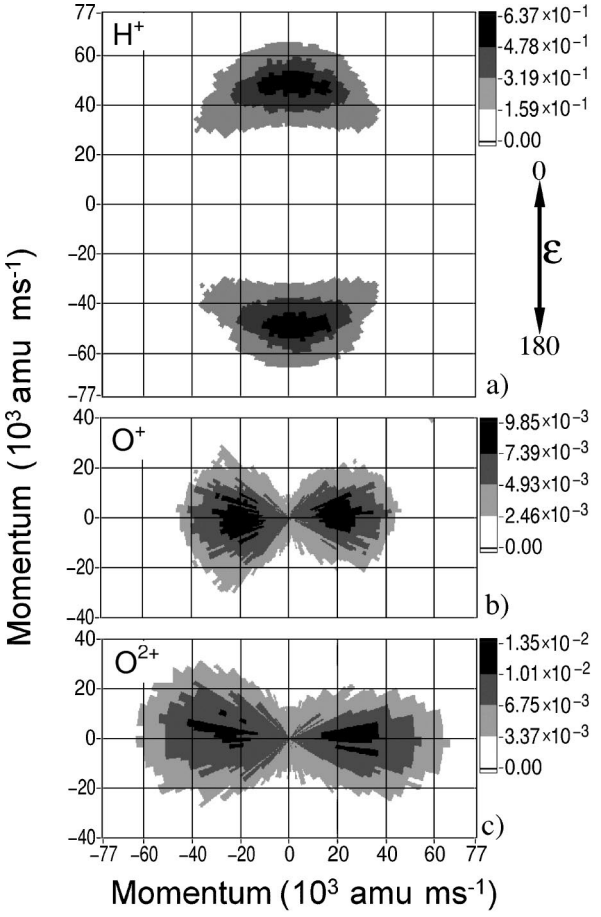

FIG. 3. Momentum maps after correction for the finite collection angle of the detector.

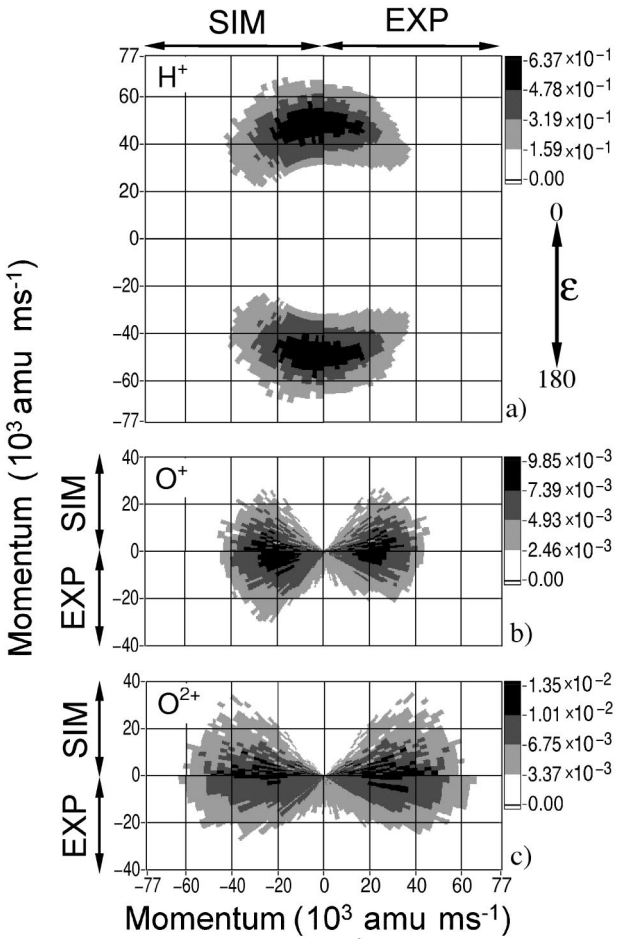

FIG. 4. Comparison between experimental (EXP) and simulated (SIM) momentum maps.

of the O^+ and O^{2+} ion intensities of Fig. 3. The simulated maps were individually normalized so that they could be compared with the experimental maps. The initial distributions chosen were consistent with the geometry of the neutral molecule, i.e., the θ distribution peaking at 104° and the R distribution peaking at 0.96 Å. These were not found to give a good agreement with the experimental map, and so were varied until the best agreement was found. Figures 4(a)–4(c) show a comparison between the experimentally derived and the best-simulated momentum maps. The general agreement is good, with the simulated maps reproducing the shape of the islands and the positions of the highest ion signal in the experimental maps.

Figures 5(a)–5(c) show the derived distributions for R, ϕ, and θ. For both channels, the R distribution was found to peak at 2 Å, in good agreement with the critical distance theory [12,13]. The alignment distribution ϕ narrows with increasing ionization channel as expected [4]. This is for two reasons: better alignment is needed between the molecule and the field to produce the higher ionization channel; and the greater field strength, which produces the higher channel, also gives rise to more reorientation. Triangular alignment distributions with full width at half maximum of 60° and 40° were derived to describe the (1,1,1) and (1,2,1) channels of CO_2 [3], as compared to 70° and 60°, respectively, in the present work. The results are therefore consistent with reorientation of H_2O, but to a lesser extent in H_2O than in CO_2, due to competition between the parallel and perpendicular torques. The maximum in the bond angle θ distribution is at 130° for the (1,1,1) channel and 140° for the (1,2,1) channel. This compares with a most probable angle of 104° for the neutral molecule; even more striking is the fact that the bend angle distributions saturate at these values. Figure 5(d) also shows a comparison with θ_V the angle between the H^+ trajectories, calculated with a multiconfigurational self-consistent-field technique [14] for dissociating H_2O^{3+} and H_2O^{4+} excited by highly charged ion impact. These distributions describe the molecular ion geometries well, but the bond angles cannot directly be derived from them, as the dissociation is not completely Coulombic. Nevertheless, the dissociation is close to Coulombic, the θ_V distributions are a good approximation to the natural bond angle distributions, and they show a low probability for large angles. In the present work the observation of high probabilities for large bond angles, between 130° and 180°, strongly indicates that the molecules have been straightened in the laser field. The phenomenon responsible for this straightening of the molecule may be bond angle softening [15], tentative evidence for which has been found in the photoelectron spectrum of H_2O at 532 nm. Figure 6 shows the interaction potential as a function of θ for the H_2O^+ ion with the $\tilde{A}\ ^2A_1$ state lowered by the photon energy of 1.6 eV. This makes the crossing positions close to the centers of the wells of the $\tilde{X}\ ^2B_1$ ground state, and close to the most probable angle for H_2O^+,

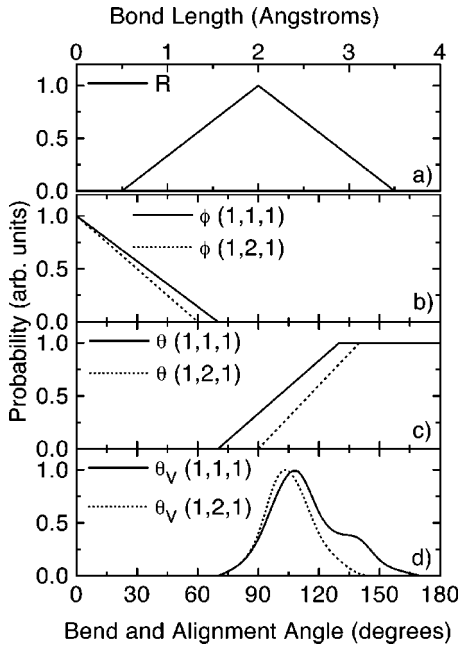

FIG. 5. Distributions of the bond length R, alignment angle ϕ, and bend angle θ used to generate the simulated map in Fig. 4. Also shown are the θ_v distributions calculated by Werner *et al.* [14]. See the text for a discussion of the single-photon process, which allows the molecule to access large bond angles, in the present experiment.

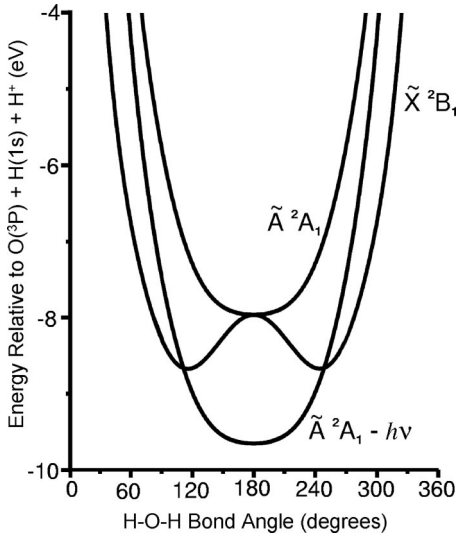

FIG. 6. Interaction potential for H_2O^+ derived from Rottke *et al.* [15], with the $\tilde{A}\ ^2A_1$ state shifted by the photon energy of 1.6 eV.

which is 120°. The process of bond angle softening occurs by a single-photon transition from the ground state onto the $\tilde{A}\,^2A_1$ state; the molecule then begins a large-amplitude oscillation to the other crossing, where it emits a photon and returns to the ground state. The time scale for this motion is comparable to the rise time of the laser pulse. If the molecule is ionized near the start of the laser pulse, which is likely, then there is enough time for the ion to undergo this bending process before the peak intensity is reached, and Coulomb explosion takes place. The bend angle distribution would be modified in this process, increasing the importance of large angles as observed.

In conclusion, using high-intensity femtosecond laser pulses, we have been able to excite the H_2O^+ molecule to high vibrational levels through a single-photon, bond angle softening process, and observe the resulting nuclear motion, through Coulomb explosion, using a momentum-mapping technique. This technique has also revealed the stretching of the bonds, before Coulomb explosion, consistent with enhanced ionization and alignment of the fragment ions, consistent with the reorientation of the molecule in the laser field. Further theoretical studies of the bond angle softening process in a high-intensity laser pulse would be beneficial.

[1] J. H. Sanderson, R. V. Thomas, W. A. Bryan, W. R. Newell, A. J. Langley, and P. F. Taday, J. Phys. B: At. Mol. Opt. Phys. **30**, 4499 (1997).

[2] C. Cornaggia M. Schmidt, and D. Normand, J. Phys. B: At. Mol. Opt. Phys. **27**, L123 (1994).

[3] C. Cornaggia, Phys. Rev. A **54**, R2555 (1996).

[4] J. H. Sanderson, R. V. Thomas, W. A. Bryan, W. R. Newell, A. J. Langley, and P. F. Taday, J. Phys. B: At. Mol. Opt. Phys. **31**, L599 (1998).

[5] J. H. Sanderson, R. V. Thomas, W. A. Bryan, W. R. Newell, I. D. Williams, A. J. Langley, and P. F. Taday, J. Phys. B: At. Mol. Opt. Phys. **31**, L59 (1998).

[6] C. Cornaggia, F. Salin, and C. Le Blanc, J. Phys. B: At. Mol. Opt. Phys. **29**, L749 (1996).

[7] H. Hishikawa, A. Iwamae, K. Hoshina, M. Kono, and K. Yamanouchi, Chem. Phys. Lett. **282**, 283 (1998).

[8] W. C. Wiley and I. H. McLaren, Rev. Sci. Instrum. **26**, 1150 (1955).

[9] J. H. Posthumus, J. Plumridge, M. K. Thomas, K. Codling, L. J. Frasinski, A. J. Langley, and P. F. Taday, J. Phys. B: At. Mol. Opt. Phys. **31**, L553 (1998).

[10] Ch. Ellert, H. Stapelfeldt, E. Constant, H. Sakhai, J. Wright, D. M. Rayner, and P. B. Corkum, Philos. Trans. R. Soc. London, Ser. A **356**, 329 (1998).

[11] V. R. Bhardwaj, C. P. Safvan, K. Vijaylakshmi, and D. Mathur, J. Phys. B: At. Mol. Opt. Phys. **30**, 8321 (1997).

[12] J. H. Posthumus, A. J. Giles, M. R. Thompson, L. J. Frasinski, K. Codling, A. J. Langley, and W. Shaikh, J. Phys. B: At. Mol. Phys. **29**, L525 (1996).

[13] T. Seideman, M. Yu. Ivanov, and P. B. Corkum, Phys. Rev. Lett. **75**, 2819 (1995).

[14] U. Werner, K. Beckord, J. Becker, H. O. Folkerts, and H. O. Lutz, Nucl. Instrum. Methods Phys. Res. B **98**, 385 (1995).

[15] H. Rottke, C. Trump, and W. Sander, J. Phys. B: At. Mol. Opt. Phys. **31**, 1083 (1998).